Journal of Translational Regenerative Medicine

2026. Volume 1

Research Paper

Developing a Novel Electrospun Nanofibrous Dressing Containing Nanostructured Lipid Carriers and *Moringa oleifera* Leaf Extract for Epidermolysis Bullosa Wounds

Elmira Banaee Mofakham[1], Saeed Hesaraki[1*], Mohammad Pazouki[2], Masoud Esfandeh[3]

1. Department of Nanotechnology and Advanced Materials, Biomaterials Group, Materials and Energy Research Centre, Alborz, Iran.
2. Department of Energy, Materials and Energy Research Centre, Karaj, Iran.
3. Department of Polymer Processing, Iran Polymer and Petrochemical Institute, Tehran, Iran.

Use your device to scan and read the article online

Citation Banaee Mofakham E, Hesaraki S, Pazouki M, Esfandeh M. Developing a Novel Electrospun Nanofibrous Dressing Containing Nanostructured Lipid Carriers and Moringa oleifera Leaf Extract for Epidermolysis Bullosa Wounds. Journal of Translational Regenerative Medicine. 2025; 1:E1016. http://dx.doi.org/10.32598/JTRM.1.1016

http://dx.doi.org/10.32598/JTRM.1.1016

ABSTRACT

Background: Epidermolysis bullosa (EB) is a rare genetic disorder characterized by severe skin fragility, necessitating specialized wound care that reduces tissue damage during dressing changes. This study aimed to fabricate and characterize a novel, electrospun nanofibrous wound dressing designed specifically for EB management.

Methods: The composite scaffold—comprising polyvinyl alcohol, carboxymethyl cellulose, gelatin, and polycaprolactone—contained *Moringa oleifera* leaf extract (MOLE), as a bioactive agent, and nanostructured lipid carriers (NLCs) to reduce cell adhesion to the dressing.

Results: The NLC-loaded scaffold with MOLE had smooth, bead-free morphology with an average fiber diameter of 190.02 nm. The addition of NLCs resulted in appropriate surface wettability (contact angle=61.3˚), maintained an ideal water vapor transmission rate of 8.55 mg/cm²h, and had suitable porosity (68.43%) and water uptake capacity (269%), ensuring a significant reduction in fibroblast adhesion, indicating the dressing's potential for atraumatic, painless removal. Furthermore, MTT and live/dead assays confirmed the scaffold's excellent biocompatibility, with high quantitative cell viability (91.9% and 87.8% on days 2 and 3, respectively) over 72 hours. Moreover, gene expression test showed a significant increase in expression of *COL7A1* gene, confirming the scaffold's potential to promote the structural regeneration of fragile skin.

Conclusion: The fabricated electrospun dressing that contained MOLE and NLCs has a great potential as a biocompatible dressing for the effective treatment and regeneration of fragile EB skin wounds.

Keywords: Epidermolysis bullosa (EB), Nanostructured lipid carriers (NLCs), Dressing, Cell adhesion

Article info:
Received: 05 Jun 2026
Accepted: 10 Jul 2026
Publish: 02 Aug 2026

*** Corresponding Author:**
Saeed Hesaraki, Professor.
Address: *Department of Nanotechnology and Advanced Materials, Biomaterials Group, Materials and Energy Research Centre, Alborz, Iran.*
E-mail: *S-hesaraki@merc.ac.ir*

Highlights

- A novel electrospun nanofibrous dressing was developed for EB wound care.
- NLCs incorporated in the dressing reduced fibroblast adhesion for atraumatic dressing removal.
- The dressing showed suitable surface wettability and moisture management.
- High biocompatibility was confirmed by cell viability above 87%.
- Upregulation of *COL7A1* gene expression indicated enhanced skin regeneration potential.

Plain Language Summary

Epidermolysis bullosa (EB) is a rare genetic disorder. The management of EB wounds requires advanced wound dressings. For this purpose, electrospun nanofibrous scaffolds are an excellent choice. This study fabricated a novel electrospun wound dressing composed of natural polymers, and containing *Moringa oleifera* leaf extract and nanostructured lipid carriers (NLCs), for the treatment of EB wounds. The dressing showed suitable surface wettability and moisture management and high biocompatibility. NLCs incorporated in the dressing reduced fibroblast adhesion for atraumatic dressing removal. The fabricated dressing has a great potential as a biocompatible dressing for the effective healing of EB wounds.

Introduction

Epidermolysis bullosa (EB) is a rare genetic disorder that, under minor mechanical stress, causes severe skin fragility and the formation of deep blisters, peeling, and erosions [1]. There are three major types of EB characterized by loss of tissue integrity in the upper dermis (simplex), in the dermal-epidermal surface (dystrophic), and within the epidermis (junctional) [2]. In severe subtypes, such as recessive dystrophic EB, the disease is primarily driven by mutations in the *COL7A* gene encoding type VII collagen (C7), leading to deficiency or dysfunction of C7 (the major component of anchoring fibrils at the dermal-epidermal junction). The management of EB wounds requires specialized, continuous care, relying heavily on advanced wound dressings to protect the compromised skin barrier, manage exudate, and promote re-epithelialization [3–5]. A critical challenge in the clinical management of EB wounds is the atraumatic removal of dressings. Traditionally, petrolatum (vaseline) or paraffin was used on the surface of the primary dressings to hinder adhesion of the dressings to the wound surface, but in some cases, secondary dressings or wound absorbent lipid components result in drying the primary dressing and increasing the adherence of the dressing to the wound [6]. Therefore, there is a compelling need for next-generation dressings that reduce tissue adhesion while maintaining optimum properties for tissue regeneration.

To address the demand for advanced wound care, electrospun nanofibrous scaffolds are an excellent choice. Through electrospinning, it is possible to fabricate breathable, highly porous mats with a high surface area-to-volume ratio that mimic the architecture of the native extracellular matrix (ECM) [7–10]. Fabrication of electrospun mats, a blend of synthetic and natural polymers—specifically polyvinyl alcohol (PVA), carboxymethyl cellulose (CMC), gelatin (Gel), and polycaprolactone (PCL)—provides an optimal balance of mechanical integrity, biocompatibility, and fluid management. To enhance the scaffold's therapeutic efficacy, bioactive agents such as *Moringa oleifera* (MO) extract can be incorporated. MO is known for its excellent antioxidant, anti-inflammatory, and antimicrobial properties, making it an ideal candidate to accelerate wound closure and prevent infection in chronic wounds [11].

Despite the structural advantages of electrospun dressings, their highly porous and hydrophilic nature can inadvertently allow cellular infiltration and strong protein adsorption from the wound exudate, leading to the enormous problem of the dressing adhering to the wound bed. To overcome this limitation and address the specific unmet clinical needs of EB patients, this study introduced a novel approach by incorporating nanostructured lipid carriers (NLCs) into a composite nanofibrous matrix. While electrospun mats provide necessary breathability, the specific addition of NLCs creates a unique surface

interface that minimizes cellular and protein attachment to the scaffold. This innovative combination ensures painless, atraumatic dressing changes for extremely fragile EB skin without compromising the dressing's exudate management capabilities [12, 13]. The main goal of this study is to fabricate and characterize a novel electrospun wound dressing composed of PVA/CMC/Gel/PCL, containing MO leaf extract (MOLE) and NLCs, specifically for the treatment of EB wounds. The effect of lipid nanoparticle incorporation on the physical and morphological characteristics of the scaffolds, including fiber size, mechanical strength, surface wettability (contact angle), water absorption capacity, and water vapor transmission rate (WVTR) is also evaluated. Furthermore, the adhesion of cells to the lipid nanoparticles incorporated into the dressing surface is assessed alongside MTT assays to confirm cellular viability and scaffold biocompatibility. Finally, to evaluate the specific regenerative potential of the optimal scaffold for EB, the expression levels of the *COL7A1* gene were measured to demonstrate the dressing's capacity to actively support the structural repair of EB wounds.

Materials and Methods

Materials

The materials used in this study included CMC (average Mw=50 KDa, degree of substitution=1.31; Kelong Chemical Co., China), gelatin powder from Bovine skin (type B; Sigma Aldrich), PVA (average Mw=72 KDa; Tetrachem Co., Iran), PCL (average MW=80 KDa; Farmed Co., Iran), phosphate buffer saline (PBS) tablets (Merck), acetic acid (AA) 99% (Dr Mojalali Co., Iran), chloroform 98% (Merck), methanol 99.5% (Baraka Co., Iran), lecithin (Baraka Co., Iran), cocoa butter (Oila Co., Iran), olive oil (Oila Co., Iran), and MO leaves (Giah Baresh, Iran). Double-distilled water was used throughout this study.

Preparation of solutions

Mixture of hydrophilic solutions containing 20% CMC (2% w/v in distilled water), 10% Gel (2% w/v in AA 80%), and 30% PVA (17% w/v in distilled water), and the hydrophobic solutions containing 30% PCL (12% w/v, dissolved in chloroform/methanol at 6:2 ratio) solution at 27 ˚C were used to produce electrospinning fibers.

To achieve lipid nanoparticles (NLCs), two phases consisting of lipid and aqueous phases were needed. In the lipid phase, it was prepared by mixing 150 mg cacao butter (as solid lipid) with 75 mg olive oil (as liquid lipid) and melting them at 40 ˚C for 5 min. In the aqueous phase, it was prepared by mixing lecithin (as surfactant) with 12.5 mL of distilled water and heating it at 40 ˚C for 10 min. Then, it was poured into the product prepared in the lipid phase under homogenization (Ultra-Turrax T25, IKA, Labortechnik, Denmark) at 24000 rpm for 5 min. After that, the resulting emulsion was cooled with 12 mL of distilled water at 4 ˚C. To avoid agglomeration, it was subjected to ultrasound (37 kHz, FAPAN Co., Iran) for 15 min. The resulting lipid nanoparticle suspension was stored at 4 ˚C until utilization [14]. The prepared NLCs (1%) was added to the hydrophilic component of the electrospinning solution.

To prepare the MOLE, MO leaves were first cleaned with distilled water and then dried at room temperature for 2 weeks. To form coarse powder with high surface area for optimal extraction, dried leaves were ground by electric blender (Bosch, Germany) and 25 g of powder was macerated with 300 mL of water for 3 days at 4 ˚C followed by filtration with filter paper (Whatman No. 1 with 11 µm pore size) and centrifuged (Fidranic Co., Iran) at 11000 rpm for 10 min to separate any solid material from aqueous solution. After that, the collected solution was stored at -20 ˚C overnight and freeze-dried (Martin Christ, Germany) for 2 days to extract MO leaves. MOLE was stored in the freezer until utilization. The MOLE (20 mg) was added to the hydrophilic part of the electrospinning solution.

The electrospinning device was from Fanavaran Nano Megyas Company (Iran). Two pumps (parallel to each other) were used for delivering aqueous solution (voltage=18.5 kV, distance=12 cm, flow rate=0.2 mL/h, rotation speed of the collector=100 rpm) and PCL solution (voltage=16 kV, distance=12 cm, flow rate=0.2 mL/h, rotation speed of the collector=100 rpm). The collected nanofibers were dried at room temperature before any characterization assays.

Characterization

Physical-chemical properties of NLCs

Polydispersity index (PI), zeta potential, and particle size (PS) of lipid nanoparticles, after suitable dilution with distilled water, were determined at room temperature at an angle of 90˚ using photon correlation spectroscopy (Brookhaven Instruments, USA). The stability of NLCs was studied for up to 90 days of storage at 4 ˚C.

Field emission scanning electron microscopy

Using field emission scanning electron microscopy (FESEM; Mira3, Tescan Co., Brno, Czech Republic) at a voltage of 20 kV, surface morphologies of NLCs were analyzed. Coating with gold sputter was performed before the analysis to increase the electrical conductivity of the nanofibers. The average diameter of the nanofibers was determined by analyzing FESEM images with an image analysis software (Image I software version 1.54k, National Institutes of Health, USA, 2025). Image analysis was performed using ImageJ software (Version 1.54k, National Institutes of Health, USA, 2025). For this purpose, 100 nanofibers were chosen randomly and analyzed [15].

Evaluation of physical and mechanical properties of fibers

Using a static contact angle measuring device (KRUSS, Hamburg, Germany), the wettability of nanofibers was determined. In this test, 10 mL drops of distilled water were poured onto three different points on the nanofibers' surface, and the mean contact angle between each sample's surface and the droplet was reported [16, 17]. According to ISO 5270:1999 standard and using a uniaxial tensile testing apparatus (Santam Co., Iran) with an extension rate of 1 mm/min, the tensile strength of the nanofibers was determined [16].

To measure the porosity of the nanofibers, the liquid displacement technique was utilized. In this test, a cylinder containing a known volume (V_1) of ethanol was used. The nanofibers with a weight of 40 mg were immersed in this cylinder. Then, the resulted volume (V_2) was evaluated. After 10 min, the nanofibers were ejected, and the volume of the residual ethanol (V_3) was recorded. Equation 1 was used to measure the porosity of the nanofibers [16]:

1. $Porosity\ (\%)=(V_1-V_3)/(V_2-V_3)\times100$

In this study, the weight of each nanofiber was first measured (W_0). Then, each of the samples was incubated in PBS solution. After 48 h, nanofibers were removed from the solution and weighed (W_1). Equation 2 was used to record the weight loss [16]:

2. $Weight\ loss\ (\%)=(W_0-W_1)/W_0\times100$

To measure the WVTR, a flexible bottle was used. In this test, 10 mL of deionized water was filled in bottles with a diameter of 13 mm, and nanofibers were capped over the circular opening of the bottle. After 24 h, the capped bottles were incubated at 33 ˚C. Equation 3 was used to estimate the WVTR (g/m^2h):

3. $WVTR=W/AT$

Where W, A, and T are the mass of water vapor transmitted, area of the mouth of the bottle, and exposure time, respectively [16].

The nanofibers were cut into 1×1 cm^2 pieces and immersed in distilled water at 27º for 1, 2, 3, 27, and 48 h. The dry weight (W_0) and the wet weight (W_1) of the nanofibers were measured after the immersion period. Equation 4 was used to estimate the water uptake capacity of nanofibers, which was repeated three times for each sample:

4. $Water\ uptake\ (\%)=(W_1-W_0)/W_0\times100$

Cell adhesion test

To investigate the adhesion of fibroblasts to the Poly(vinyl alcohol)/carboxymethyl cellulose/gelatin/*M. oleifera* leaf extract/polycaprolactone (PCGMPCL) and the poly(vinyl alcohol)/carboxymethyl cellulose/gelatin/*M. oleifera* leaf extract/lipid nanoparticles/polycaprolactone scaffold (PCGMNPCL) nanofibers, celladhesion test was used. Briefly, dressings were affixed to the bottom of 24-well plates using 10 µL of fibrin as an adhesive. After incubation for 30 min and formation of a fibrin clot, fibroblasts at a density of 100000 cells/ well were seeded on top of them and incubated for 12 h to allow cell attachment to the dressings. After that, by using a 2.5% glutaraldehyde solution, fibroblasts were fixed and dehydrated in graded ethanol series and finally, the images of dressings were taken by SEM device (Tescan, Brno, Czech Republic) [6].

MTT assay

The MTT colorimetric assay (Sigma, St. Louis, Mo, USA) was used to evaluate cell viability in the presence of the PCGMNPCL dressing on days 2 and 3. To perform this test, L29 fibroblasts cells were first cultured in Dulbecco-modified Eagle medium (DMEM; Gibco-BRL, Life Technologies, Japan), 100 g/mL penicillin and streptomycin (Gibco-BRL, Life Technologies, Japan) and 10% fetal bovine serum (FBS; Dainippon Pharmaceutical, Japan). Then, they were incubated in an atmosphere containing 5% CO_2. The PCGMNPCL mats were cut into circular shapes and placed in the 24-well plates (NUNC; Rochester, USA). The dressing was sterilized

for 20 min by UV irradiation. Cultured cells at a density of 50×10^4 cells/well were seeded on the dressing in 24-well plates, and 200 µL of growth medium was added to each well. The disks containing the culture dish were utilized as control samples. The cell-seeded specimens in the culture medium (24-well culture plate) were incubated in a humidified atmosphere containing 5% CO_2 at 37 ˚C for 48 h. After incubation, the medium was removed, and the plate was washed with PBS to remove residues. After that, 200 µL of fresh medium and 100 µL of MTT solution were introduced to the samples. This step was done in a dark environment. Next, plates were covered with aluminum foil and incubated in a humidified atmosphere containing 5% CO_2 at 37 ˚C for 4 h. After discarding the supernatant, 1 mL of dimethyl sulfoxide solution (DMSO) was added and the plates were vibrated for 15 min to dissolve the formazan crystals formed by viable cells. Finally, 100 µL of the solution from each well was transferred to 96-well plates, and the absorbance at 570 nm was measured by the Glomax multi-detection system microplate reader. The cells cultured without dressings were utilized as a control.

The viability of cells was also evaluated by live/dead staining of L929 fibroblasts with acridine orange (Merck) and propidium iodide (Sigma-Aldrich). As previously clarified, fibroblasts were cultured in DMEM for 24 h. After that, dressings were placed in the wells, followed by changing the medium and washing with PBS three times, and incubating for another 72 h. Loaded cells were stained with a mixture of 5 µM Acridine orange and propidium iodide in 10 mL of culture medium to determine the existence of live (green) and dead (red) cells. After incubating for 30 min, photographs were taken by Olympus fluorescent microscope (Olympus, CKX53) [18].

Gen expression

Human dermal fibroblasts (HDFs; cell number: IBRC C10506) were purchased from Bon Yakhte (Tehran, Iran). Cells were cultured in high glucose DMEM/F-12 Medium (Gibco-Invitrogen) supplied by 10% FBS (Gibco-Invitrogen) and 1% penicillin/streptomycin (Sigma-Aldrich). The cells were stored in a humidified atmosphere containing 5% CO_2 at 37 ˚C. When the cells reached more than 80% of confluency, they were detached with 0.25% trypsin and seeded in 24-well plates. The cells were randomly divided into three experimental groups: (i) control group, in which cells were cultured without a nanofibrous dressing; (ii) PCGNPCL group, in which HDFs were cultured in the presence of blank PCGNPCL nanofibrous dressing without MOLE; and (iii) PCGMNPCL group, in which HDFs were cultured in the presence of PCGMNPCL nanofibrous dressing with MOLE. Following seeding, HDFs were incubated under standard culture conditions to allow for cell attachment and stabilization. The culture medium was changed every 48–72 h during the incubation period. Cells were subsequently cultured until reaching the appropriate confluency required for molecular analyses.

Cells were harvested from differentiating plates, and the total RNA was isolated from triplicate samples by TRIzol (Yekta Tajhiz Co., Iran) in accordance with the manufacturer's protocol [19] and quantitatively measured by a spectrophotometer (Thermo Scientific, Nanodrop 1000, USA). RNA purity was assessed using the A260/A280 absorbance ratio. Extracted RNA was used to synthesize cDNA according to the instructions in the cDNA Synthesis Kit (Pars Tous Co., Iran) [20]. The Light Cycler 480 system (Roche, Germany) was used to measure reverse-transcribed cDNA with the SYBR Green PCR Kit (QIAGEN, China) under the following conditions: pre-denaturation at 95 ˚C for 5 minutes, denaturation at 95 ˚C for 10 seconds, and annealing and extension at 60 ˚C for 30 seconds. Amplification was performed for 40 cycles. The expression level of the *COL7A1* gene was determined by quantitative real-time PCR and normalized to *GAPDH* (housekeeping endogenous control). Melting curve analysis was performed at the end of amplification to confirm amplification specificity and absence of primer-dimer formation. All experiments were performed in triplicate.

Statistical analysis

All experiments, including mechanical test, cell viability test, and gene expression assay, were performed in triplicate. Quantitative data were expressed as Mean±SD. Statistical significance between experimental groups was evaluated using a one-way analysis of variance (ANOVA) followed by Tukey's post hoc test. $P<0.05$ was considered statistically significant.

Results

Physical-chemical properties of NLCs

Table 1 demonstrates PI, zeta potential, and PS of lipid nanoparticles one day and 80 days after production. The PS, zeta potential, and its distribution are very crucial factors in the stability of colloid systems. As shown in Table 1, the PS of NLCs on the first day and on day 80 after production was 166.77±29.31 nm and 327.95±12.32 nm, respectively. This shows that increasing the storage

Table 1. PI, zeta potential, and PS values of NLCs on days 1 and 80 after preparation

Day	Mean±SD		PI
	Zeta Potential (mV)	PS (nm)	
1	47.81±0.78	166.77±29.31	0.237±0.025
80	29.60±1.34	327.95±12.32	0.216±0.023

time caused the particles to aggregate. The PI value illustrates the homogeneity of the PS distribution in a given system. Ideally, PI value should be less than 0.3 to achieve a narrow size distribution of particles in a system [21]. As shown in Table 1, for NLCs on the first day and day 80, PI values were 0.237±0.025 and 0.216±0.023, respectively. Thus, the PI value remained within 0.2 after 80 days of storage, indicating that the prepared NLCs had a narrow size distribution.

The zeta potential describes the physical stability of NLCs. If electrostatic repulsion dominates the attractive Van der Waals forces, the system can be considered as stable. Generally, when the zeta potential is above 60 mV, the colloidal system is in an excellent, physically stable state; a value above 30 mV indicates that the colloidal system is physically stable; a value above 15 mV demonstrates that the colloidal particles may have aggregation; and a value below 5 mV represents sever aggregation in the colloidal particles [22]. As shown in Table 1, the zeta potential for NLCs on the first day and day 80 were 47.81±0.78 and 29.60±1.34 mV, respectively. Thus, on the first day after preparation, the NLCs were more physically stable than on day 80. On day 80, the zeta potential value decreased, but it was still near 30 mV, indicating NLCs' good physical stability. After 80 days, however, a little aggregation in particles might occur due to the increase in PS (on day 80).

Field emission scanning electron microscopy

Figure 1 shows FESEM images of nanofibers from the PCGMPCL and PCGMNPCL groups, indicating that smooth, bead-free fibers can be obtained by electrospinning solutions. The porous structure of these mats makes them suitable for wound-dressing applications, as they transmit oxygen and water vapor while maintaining wound-area moisture and temperature at levels that support faster wound healing [8, 23]. Mean diameter of the fibers in PCGMPCL and PCGMNPCL groups was 183.02 and 190.02 nm, respectively (Table 2).

It was observed that adding NLCs to the electrospinning solution causes an increase in the mean diameter of nanofibers. This slight increase in fiber diameter can be attributed to the altered viscosity and the presence of lipid droplets within the electrospinning solution. Consequently, the enlarged fiber diameter and the presence of hydrophobic lipid domains on the fiber surface directly influence the overall scaffold performance. Specifically,

Table 2. Physical and mechanical properties of nanofibers in the groups with wound dressing

Parameter	Mean±SD	
	PCGMPCL Group	PCGMNPCL Group
Mean diameter (nm)	183.02±58.75	190.02±43.45
Tensile strength (MPa)	0.49±0.77	0.39±0.32
Module (MPa)	1.39±0.13	1.35±0.43
WVTR (mg/cm^{2}h)	8.62±0.47	8.55±0.23
Degradation rate (%)	41.8±1.84	38±2.3
Contact angle (degree)	57.8±2.7	61.3±1.4
Porosity (%)	72.33±1.61	68.43±2.3

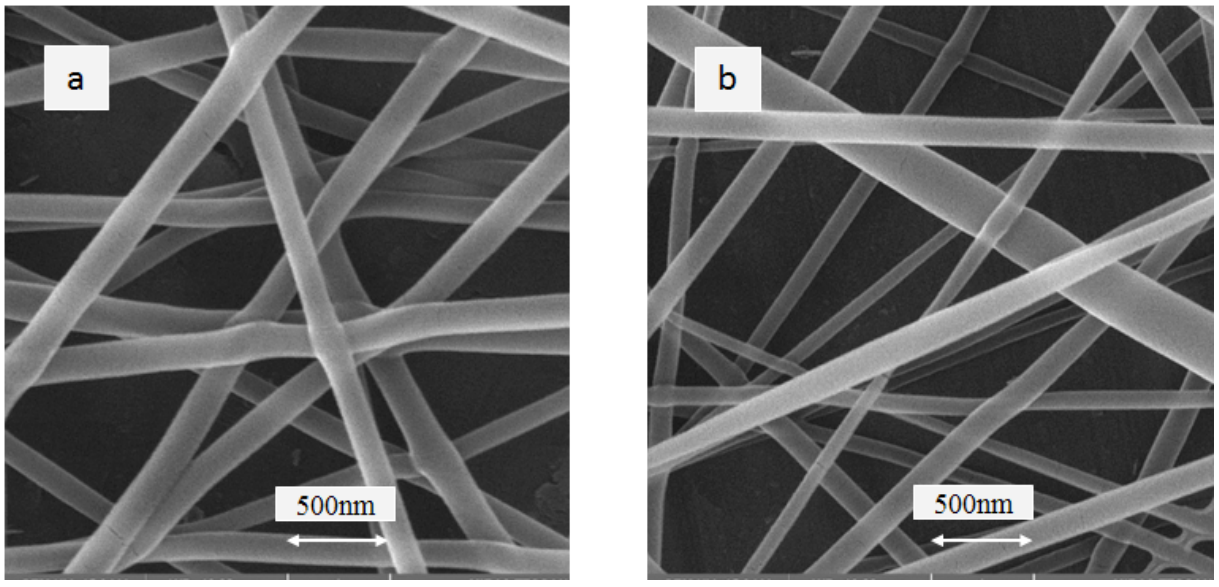

Figure 1. FESEM images of nanofibers

a) PCGNPCL, b) PCGMNPCL

thicker fibers can slightly reduce overall pore size and porosity, while morphological changes and lipid distribution enhance surface hydrophobicity. This altered physical topography and chemical composition work synergistically to reduce initial protein adsorption, thereby effectively decreasing excessive fibroblast adhesion. Obtained nanofibers are suitable for wound dressings because they mimic extracellular matrix architecture, which helps anchor cells during the cellular regeneration step of wound healing [8, 23, 24].

Physical and mechanical properties of nanofibers

One of the key factors of a suitable wound dressing is its hydrophilicity, which determines the ability of the dressing to absorb wound exudate and retain wound bed moisture [25]. The ideal contact angle for a proper wound dressing is 40-70° degrees, which promotes cell adhesion and the wound healing process [17]. The results of the surface wettability test for nanofibers in the PCGMPCL and PCGMNPCL groups are presented in Table 2. The use of NLCs (due to their hydrophobic nature) in mats increased the contact angle from 57.8° to 61.3°. These values fall within the ideal range, making them useful for exudate absorption, moisture retention, and regulation of cell adhesion during the wound-healing process [17]. Furthermore, this slight increase in contact angle following lipid nanoparticle incorporation are consistent with the findings of Garcia-Orue et al. [6], who reported similar shifts in surface wettability for electrospun membranes containing lipid nanoparticles. This controlled hydrophobicity is crucial for preventing excessive dressing adhesion while maintaining fluid management capabilities.

The mechanical properties of wound dressing materials play an important role in the wound healing process. During this process, the tensile strength and flexibility of these materials should be enough to stand firm against the handling and replacement, and facilitate cell adhesion and spreading, ECM secretion and proliferation and/or differentiation. Also, it should have enough flexibility to adapt to the wounds in folding areas and various joints. Additionally, the integrity of dressings should be assessed to prevent contamination of the wound bed by dressing fragments [24-28]. The ultimate tensile strength (MPa) and Young's modulus (MPa) values for the electrospun mats are reported in Table 2. Adding NLCs caused a decrease in both ultimate tensile strength (0.49 to 0.39 MPa) and Young's modulus (1.39±0.13 to 1.35±0.43 MPa). According to the literature, the human skin's Young's modulus is in the range of 0.01-50 MPa. Therefore, the nanofibers' Young's modulus was within this range. The ultimate tensile strength of the NLC-loaded mats (0.39 MPa) in our study is highly comparable to other recently reported electrospun composite dressings designed for soft tissue regeneration. Recent studies indicate that a tensile strength of 0.2-0.5 MPa is optimal for clinically effective skin substitutes, as it prevents mechanical trauma to the fragile wound bed [29]. While incorporating lipid nanoparticles slightly softens the scaffold (reducing tensile strength from 0.49 to 0.39

MPa), this structural flexibility is actively desired for EB patients. It maintains sufficient structural integrity to withstand handling while avoiding the stiffness that could cause friction blisters, closely matching the biomechanical behavior of native soft tissues [30]. Previous studies have demonstrated that in tissue-engineered skin applications, soft matrices promote faster cell migration than stiff ones, confirming that the developed nanofibers are structurally optimal for EB wound dressing applications [24].

The porosity of dressings is essential for oxygen and nutrient delivery to the wound area. According to studies, the best range for wound dressing porosity is 60-90% [24]. The porosity of the PCGMPCL and PCGMNPCL mats was estimated by the liquid displacement method and recorded in Table 2. Their porosity were 72.33±1.61 and 68.43±2.3%, respectively. These values are high enough (>60%) for wound-dressing applications and are highly consistent with porosities (65-75%) reported in the literature for other PVA- and PCL-based composite electrospun scaffolds designed for skin tissue engineering [8, 27]. This porous network ensures optimal gas exchange and nutrient delivery without compromising the structural integrity required for EB wounds.

The degradation rate of nanofibers in the PCGMPCL and PCGMNPCL groups is provided in Table 2. Results indicate that introducing NLC to nanofibers diminishes the degradation rate of mats from 41.8 to 38% (due to dissolution of hydrophilic parts of nanofibers) after 48 h of immersion in PBS. The dissolved hydrophilic parts of mats are the best choice for delivering active agents like drugs, antibacterial agents, and extracts to the wound site. In this study, MOLE was entrapped in soluble nanofibers, and upon dissolution in PBS, it is released to the wound site. One of the vital points of the proper wound dressing is its stability in the wound medium. When the dressing maintains its integrity (in the wound site), it would not lose its absorptive capacity during utilization and support the wound for longer periods of time. Hence, in this study, using the PCG2NMPCL sample yielded the most stable nanofiber.

During the inflammatory phase of the wound healing process, wounds produce a large amount of exudate, which promotes microbial infections. To absorb and remove excess fluid and exudate without drying the wound, wound dressings are used [28]. The vapor transition through the dressing is an important feature that directly affects the wound healing process [31]. Wounds need to maintain some level of moisture to promote collagen synthesis and angiogenesis and prevent cellular dehydration [24]. It has been reported that a dressing is considered moisture-retentive when it maintains a WVTR in the range of 8.33-10.42 mg/(cm^2 h) [8]. Higher WVTR accelerates dehydration, leading to scar formation at the wound site, while lower WVTR increases the risk of infection and delays wound healing due to exudate deposition [26]. In this study, the WVTRs of the nanofibers in the PCGMPCL and PCGMNPCL groups were 8.62 and 8.55 mg/cm^{2}h, respectively (Table 2), which are within the appropriate range for an ideal dressing. These WVTR values are highly comparable to those of other recently developed natural/synthetic electrospun mats, such as PVA/cellulose acetate scaffolds [8], ensuring efficient moisture management that prevents maceration in moderate to highly exuding wounds. The slight reduction in WVTR in the presence of NLCs may be due to the lower porosity and the hydrophobic nature of the lipid domains within the PCGMNPCL mats.

The capability of mats to eliminate exudates from the wound site is studied by the water uptake percentage. Figure 2 denotes the percentage of water uptake for the nanofibers in the PCGMPCL and PCGMNPCL groups at 1, 2, 3, 27, and 48 h after immersion in water. Results show that, as time passed, the percentage of water uptake in both groups increased, reaching 303% and 269% for PCGMPCL and PCGMNPCL nanofibers, respectively, indicating that both mats have the ability to absorb exudate. The PCGNMPCL sample had lower water-uptake capacity than PCGMPCL due to the NLCs' hydrophobic nature.

Cell adhesion

Adhesion of cells to the dressing is one of the challenges of wound dressing use [14]. To evaluate whether cells were able to adhere to nanofibers or not, they cultured on top of the PCGMPCL and PCGMNPCL dressings and SEM images were analyzed. These images were used to evaluate the effect of NLCs on cell adherence to the dressing. According to Figure 3, adhesion of cells in the PCGMNPCL sample was significantly lower than that in the PCGMPCL sample. This reduction is directly attributed to the physicochemical and topographical modifications induced by the NLCs. The incorporation of these lipid nanoparticles creates localized hydrophobic lipid domains on the predominantly hydrophilic surface of the PVA/CMC/Gel fibers. This change is quantitatively supported by the increase in the surface contact angle from 57.8° to 61.3°. This enhanced surface hydrophobicity, along with a slightly altered physical topography (increased fiber diameter), synergistically hinders the initial adsorption of adhesive proteins from the wound

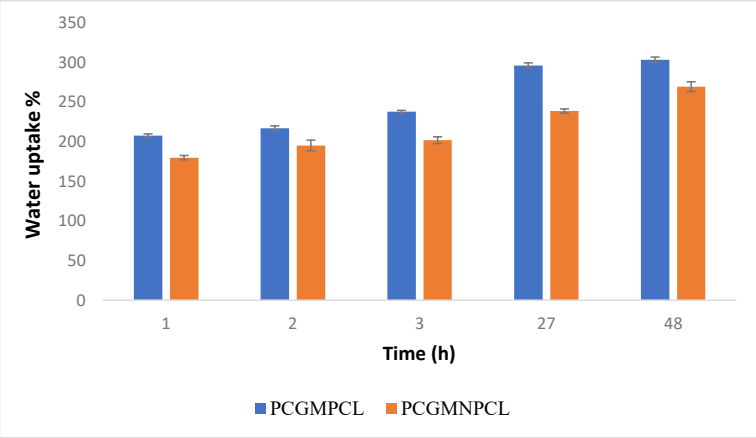

Figure 2. Water uptake percentage of nanofibers in the PCGMPCL and PCGMNPCL groups

exudate. Since protein adsorption is a fundamental prerequisite for subsequent cellular attachment, its minimization effectively reduces excessive fibroblast anchoring to the scaffold. Improved handling, ease of removal, and avoidance of pain and damage to the newly formed epidermal tissue in EB patients are the main reasons for adding NLCs to the nanofibers [6]. More research should be done to evaluate dressing attachment to the wound, either by analyzing dressing removal in vivo or by using a texture analyzer to estimate adhesion strength to the wound.

MTT assay

The use of biomaterials and chemical factors affects cell viability. Hence, it is essential to evaluate their cytotoxicity. The MTT assay method was used to estimate the cytotoxicity of the PCGMNPCL mats on days 2 and 3. Figure 4A shows the MTT assay results for PCGMNPCL and control samples. The cell viability of the control sample on days 2 and 3 was 99.93% and 100.4%, respectively, while for PCGMNPCL, it was 91.9% and 87.8%, respectively. These results demonstrate that PCGMNPCL mats are non-toxic to fibroblast cells and can be a good choice for wound-dressing applications.

Live/dead staining of fibroblast cells was performed to visualize cell viability by assessing the dispersal of live and dead cells after 72 h of incubation. Figure 4B depicts the viability of L929 fibroblast cells in the control and PCGMNPCL samples. As shown, about 2% of dead cells are observed in contact with PCGMNPCL mats, and a high number of live cells are present in both control and PCGMNPCL samples.

Gene expression

The regenerative potential of the PCGMNPCL sample was evaluated by measuring *COL7A1* gene expression in HDFs after treatment with the PCGMNPCL dressing. The results are plotted in Figure 5. The PCGMNPCL sample showed significantly higher *COL7A1* expression than the other samples. One-way ANOVA results revealed a statistically significant effect ($P<0.001$). Both PCGNPCL and PCGMNPCL treatments significantly upregulated gene expression compared to the control sample. Notably, the group with both dressing and MOLE exhibited the highest *COL7A1* gene expression, suggesting a potential synergistic effect of MOLE on *COL7A1* expression. This indicates that the bioactive compounds in MOLE affect fibroblast activity, and the extracellular matrix-related regeneration pathways increase by the upregulation of *COL7A1*, which is a component of the basement membrane and critical for dermal–epidermal adhesion and tissue integrity. Additionally, the nanofibrous structure of the PCGNPCL scaffold may create a biomimetic microenvironment conducive to cell adhesion, proliferation, and gene expression, which collectively indicate the therapeutic potential of the developed dressing for advanced wound healing and skin tissue engineering applications. Therefore, the fabricated nanofibers containing MOLE can be good choice for treatment of EB wounds.

Discussion

The present research successfully developed a novel electrospun nanofibrous wound dressing composed of PVA/CMC/Gel/PCL, incorporated with MOLE and NLCs for potential application in EB wound management. The obtained results declared that the fabricated dressing possessed suitable physicochemical, biologi-

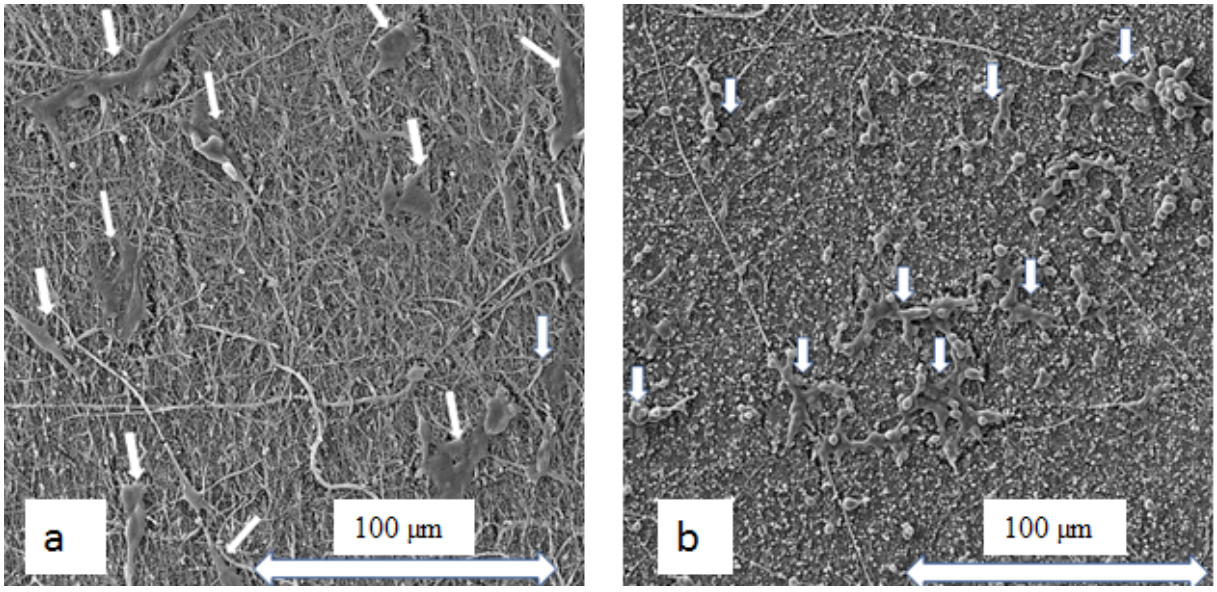

Figure 3. SEM images of cultured cells on dressings

a) PCGMPCL, b) PCGMNPCL

cal, and regenerative properties required for the treatment of fragile EB skin [32]. The combination of electrospun nanofibers with lipid nanoparticles provided a multifunctional platform capable of maintaining wound moisture, supporting tissue regeneration, and reducing traumatic adhesion during dressing removal.

Electrospinning technology enables the fabrication of nanofibrous matrices that structurally resemble the native extracellular matrix, thereby facilitating cellular interactions and tissue repair. In the present study, FESEM analysis confirmed the successful formation of smooth and bead-free fibers with nanoscale diameters. The addition of NLCs slightly increased fiber diameter, which may be related to the increased viscosity and altered conductivity of the electrospinning solution. Similar observations have been reported in previous studies evaluating lipid nanoparticle-loaded electrospun scaffolds for wound healing applications [33, 34]. The porous architecture of the fabricated mats is highly advantageous, as it enables oxygen exchange and nutrient diffusion while maintaining a moist microenvironment that accelerates wound healing.

An ideal wound dressing should have appropriate surface wettability and moisture management characteristics. The contact angle values obtained in this study remained within the optimal range for wound healing applications [35]. Although incorporating NLCs slightly increased the contact angle due to their hydrophobic nature, the dressing still maintained adequate hydrophilicity for exudate absorption and cellular compatibility. Controlled surface hydrophobicity is particularly beneficial in EB wound care applications because it can reduce excessive protein adsorption and subsequent tissue adherence while still permitting sufficient moisture retention. Moreover, the WVTR values of the fabricated dressings were within a range ideal for wound dressings, indicating the capability of the scaffold to preserve wound hydration while preventing excessive dehydration or exudate accumulation. The water uptake results further confirmed the ability of the nanofibrous mats to absorb wound exudates efficiently. Although NLC incorporation reduced water uptake due to lipid hydrophobicity, the resulting absorption capacity remained appropriate for wound management applications.

Mechanical flexibility is another critical requirement for EB wound dressings because rigid materials may cause additional skin trauma and blister formation. The fabricated nanofibers demonstrated Young's modulus values within a range reported for native human skin, indicating appropriate flexibility and elasticity. Although NLC incorporation slightly reduced tensile strength and modulus, this reduction may be advantageous for EB wound care by producing a softer and more compliant scaffold. Previous reports have shown that softer matrices can better support cellular migration and adaptation to irregular wound surfaces [36]. Therefore, the developed scaffold may effectively conform to fragile EB skin while minimizing friction-induced damage.

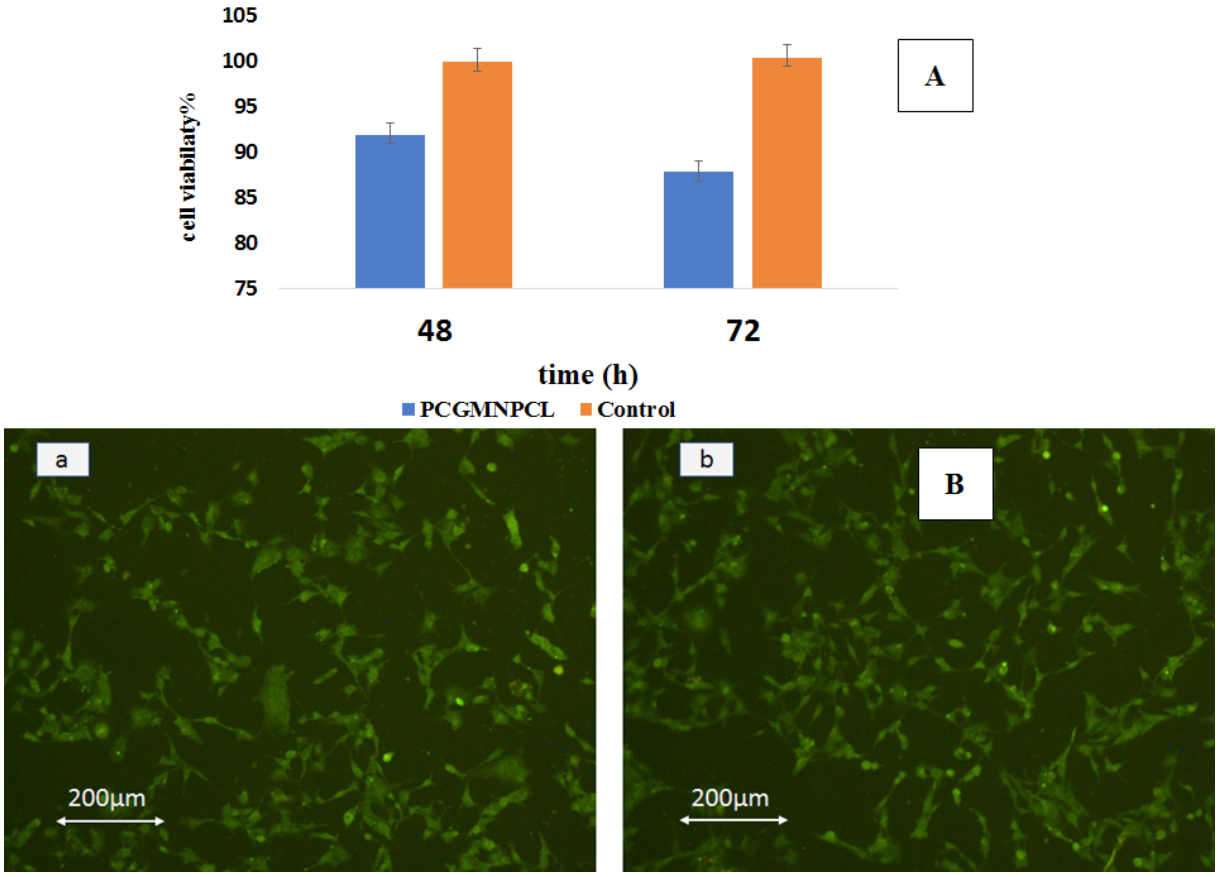

Figure 4. Water absorption of the samples as a function of time

A) Histogram of MTT assay for PCGMNPCL and control samples at 48 and 72 h, B) Live/dead staining images showing the viability of L929 fibroblast cells in (a) control and (b) PCGMNPCL samples

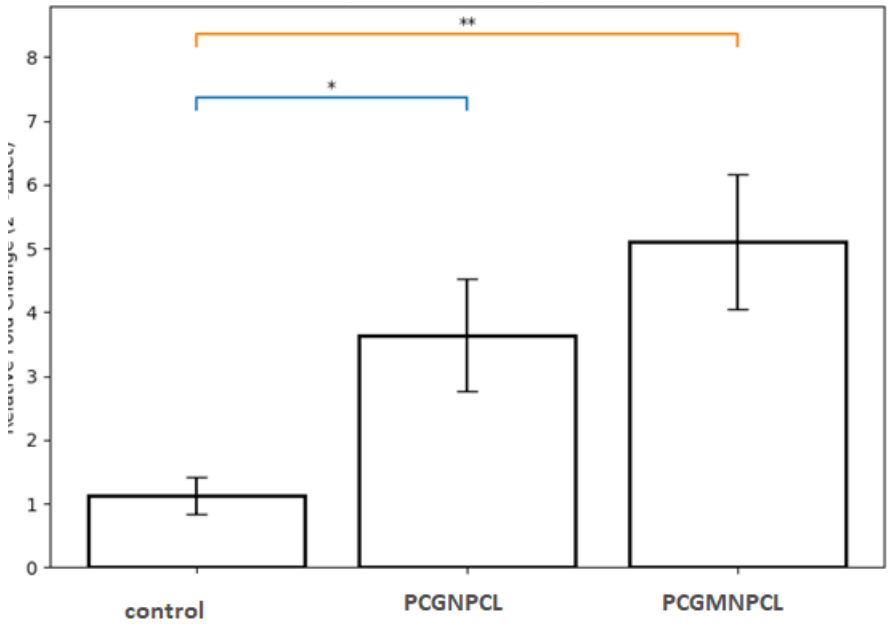

Figure 5. *COL7A1* gene expression in three groups

*P<0.05, **P<0.01.

One of the major clinical challenges in EB wound treatments is the painful dressing removal caused by dressing adherence to the wound surface. The present study demonstrated that the incorporation of NLCs significantly reduced fibroblast adhesion to the scaffold surface. This reduction may be attributed to the combined effects of increased hydrophobicity, altered surface topography, and reduced protein adsorption induced by lipid nanoparticles. Since protein adsorption is an essential initial step in cellular attachment, reduced protein interactions can minimize excessive cell anchorage to the dressing. Consequently, the fabricated dressing may facilitate painless and atraumatic removal, which is highly important for improving the quality of life in EB patients.

Biocompatibility evaluation demonstrated that the fabricated dressing was non-toxic to fibroblast cells. MTT assay and live/dead staining demonstrated high cell viability and minimal cell death after exposure to the scaffold. These results confirm that the selected polymers, lipid nanoparticles, and MOLE did not have cytotoxic effects on fibroblasts. The favorable cellular response may be associated with the intrinsic biocompatibility of PVA, gelatin, CMC, and PCL, as well as the bioactive compounds present in MOLE. Previous studies have reported that MO contains antioxidant and anti-inflammatory phytochemicals that can promote fibroblast proliferation and accelerate tissue repair [37].

Importantly, the gene expression analysis showed significant upregulation of *COL7A1* gene expression in cells treated with the MOLE-containing scaffold. COL7A1 is the primary structural component of anchoring fibrils at the dermal–epidermal junction and plays a crucial role in maintaining skin integrity. Since mutations and deficiencies in COL7A1 are directly associated with dystrophic EB, the observed increase in *COL7A1* gene expression suggests that the fabricated scaffold may actively contribute to structural skin regeneration. The enhanced expression observed in the MOLE-containing group may be related to the synergistic effects of the nanofibrous microenvironment and the biological activity of MOLE phytochemicals on fibroblast function and extracellular matrix synthesis. Therefore, beyond serving as a passive wound covering, the developed dressing may possess regenerative therapeutic potential for EB wound treatment.

Despite the promising findings, this study had several limitations. The anti-adhesion performance of the dressing was only evaluated in vitro using fibroblast adhesion assays. Future investigations should include in vivo wound models and quantitative measurements of adhesion force to better assess painless dressing removal under clinical conditions. Additionally, long-term biological performance and in vivo wound healing efficacy should be examined before clinical translation.

Overall, the developed PCGMNPCL nanofibrous dressing revealed favorable structural, mechanical, biological, and regenerative properties for EB wound care. The combination of electrospun nanofibers, NLC-mediated anti-adhesive functionality, and MOLE bioactivity offers a promising strategy for developing next-generation wound dressings tailored to fragile skin disorders such as EB.

Conclusion

In this study, a novel electrospun nanofibrous wound dressing composed of PVA/CMC/Gel/PCL, loaded with MOLE and NLCs, was successfully fabricated to help the critical challenges of EB wound care. The fabricated scaffolds highly mimic the native extracellular matrix. Despite the incorporation of NLCs, the Young's modulus (1.35 MPa) remained perfectly aligned with the mechanical requirements of human skin. The dressing exhibited a sufficient porosity (68.43%), an ideal WVTR (8.55 mg/cm²h), and excellent water uptake capacity (269%). These characteristics ensure that the wound bed remains adequately moisturized while preventing excessive exudate accumulation, which is essential for preventing microbial infections. SEM imaging confirmed that NLCs actively reduced fibroblast adhesion to the scaffold, thereby enabling painless, non-destructive dressing changes and providing a solution to the long-standing clinical problem of dressing adherence in EB patients. MTT and live/dead assays confirmed that the dressing was highly biocompatible and non-toxic, supporting cell viability over 3 days. The significant enhancement of *COL7A1* gene expression further highlights the MOLE-containing nanofibers' capacity to actively improve tissue integrity and promote structural wound healing. The PCGMNPCL dressings appear to be an excellent option for the treatment of EB wounds, serving as a highly viable next-generation therapeutic dressing for severe genetic skin blistering disorders.

Compliance with ethical guidelines

There were no ethical considerations to be considered in this research.

Funding

The present paper was extracted from the PhD dissertation of Elmira Banaee Mofakham, approved by the Material and Energy Research Center, Karaj, Iran.

This research was financially supported by the Materials and Energy Research Center, Karaj, Iran, and the Iran Polymer and Petrochemical Institute (IPPI), Tehran, Iran.

Authors' contributions

Conceptualization: Elmira Banaee, Saeid Hesaraki, and Mohammad Pazouki; Methodology, software, formal analysis investigation, and data curation: Elmira Banaee and Saeid Hesaraki; Validation: Elmira Banaee, Saeid Hesaraki, and Mohammad Pazouki; Resources and funding acquisition: Saeid Hesaraki, Mohammad Pazouki, and Masoud Esfandeh; Writing the original draft, and visualization: Elmira Banaee; Review and editing: All authors; Project administration: Saeid Hesaraki. Supervision: Saeid Hesaraki and Mohammad Pazouki.

Conflict of interest

The authors declared no conflict of interest.

Acknowledgments

The authors would like to express their sincere gratitude and appreciation to all individuals and organizations for their support and contributions to this study.

References

[1] Has C, Bauer JW, Bodemer C, Bolling MC, Bruckner-Tuderman L, Diem A, et al. Consensus reclassification of inherited epidermolysis bullosa and other disorders with skin fragility. British Journal of Dermatology. 2020; 183(4):614-27. [DOI:10.1111/bjd.18921] [PMID]

[2] Sadighi T, Swayne C. Epidermolysis bullosa simplex: Disorder of tissue fragility. Journal of the Dermatology Nurses' Association. 2022; 14(1):16-9. [Link]

[3] Uitto J, Bruckner-Tuderman L, Christiano AM, McGrath JA, Has C, South AP, et al. Progress toward treatment and cure of epidermolysis bullosa: Summary of the DEBRA international research symposium EB2015. The Journal of Investigative Dermatology. 2016; 136(2):352-8. [DOI:10.1016/j.jid.2015.10.050] [PMID] [PMCID]

[4] Bardhan A, Bruckner-Tuderman L, Chapple ILC, Fine J, Harper N, Has C, et al. Epidermolysis bullosa. Nature Reviews Disease Primers. 2020; 6: 78. [DOI: 10.1038/s41572-020-00220-7]

[5] Marwah MK, Kaur K, Ahmad S, Cheema HCK. Innovations in topical epidermolysis bullosa treatment: integrating advanced dressings, bioactive therapies and tissue-engineered skin. Daru 2026; 34(1):22. [DOI:10.1007/s40199-026-00601-5] [PMID] [PMCID]

[6] Garcia-Orue I, Gainza G, Garcia-Garcia P, Gutierrez FB, Aguirre JJ, Hernandez RM, et al. Composite nanofibrous membranes of PLGA/Aloe vera containing lipid nanoparticles for wound dressing applications. International Journal of Pharmaceutics. 2019; 556:320-9. [DOI:10.1016/j.ijpharm.2018.12.010] [PMID]

[7] Sultana N, Zainal A. Cellulose acetate electrospun nanofibrous membrane: Fabrication, characterization, drug loading and antibacterial properties. Bulletin of Materials Science. 2016; 39:337-43. [DOI:10.1007/s12034-016-1162-6]

[8] Gaydhane MK, Kanuganti JS, Sharma CS. Honey and curcumin loaded multilayered polyvinylalcohol/cellulose acetate electrospun nanofibrous mat for wound healing. Journal of Materials Research. 2020; 35:600-9. [DOI:10.1557/jmr.2020.52]

[9] Liu X, Lin T, Gao Y, Xu Z, Huang C, Yao G, et al. Antimicrobial electrospun nanofibers of cellulose acetate and polyester urethane composite for wound dressing. Journal of Biomedical Materials Research. Part B, Applied Biomaterials. 2012; 100(6):1556-65. [DOI:10.1002/jbm.b.32724] [PMID]

[10] Tomar Y, Pandit N, Priya S, Singhvi G. Evolving trends in nanofibers for topical delivery of therapeutics in skin disorders. ACS Omega. 2023; 8(21):18340-57. [DOI:10.1021/acsomega.3c00924] [PMID] [PMCID]

[11] Gothai S, Arulselvan P, Tan WS, Fakurazi S. Wound healing properties of ethyl acetate fraction of Moringa oleifera in normal human dermal fibroblasts. Journal of Intercultural Ethnopharmacology. 2016; 5(1):1-6. [DOI:10.5455/jice.20160201055629] [PMID] [PMCID]

[12] Puri D, Bhandari A, Sharma P, Choudhary D. Lipid nanoparticles (SLN, NLC): A novel approach for cosmetic and dermal pharmaceutical. Journal of Global Pharma Technology. 2010; 2(9):1-5. [Link]

[13] Farasati Far B, Naimi-Jamal MR, Sedaghat M, Hoseini A, Mohammadi N, Bodaghi M. Combinational system of lipid-based nanocarriers and biodegradable polymers for wound healing: An updated review. Journal of Functional Biomaterials. 2023; 14(2):115. [DOI:10.3390/jfb14020115] [PMID] [PMCID]

[14] Saporito F, Sandri G, Bonferoni MC, Rossi S, Boselli C, Icaro Cornaglia A, et al. Essential oil-loaded lipid nanoparticles for wound healing. International Journal of Nanomedicine. 2017; 13:175-86. [DOI:10.2147/IJN.S152529] [PMID] [PMCID]

[15] Gomaa SF, Madkour TM, Moghannem S, El-Sherbiny IM. New polylactic acid/ cellulose acetate-based antimicrobial interactive single dose nanofibrous wound dressing mats. International Journal of Biological Macromolecules. 2017; 105(Pt 1):1148-60. [DOI:10.1016/j.ijbiomac.2017.07.145] [PMID]

[16] Samadian H, Zamiri S, Ehterami A, Farzamfar S, Vaez A, Khastar H, et al. Electrospun cellulose acetate/gelatin nanofibrous wound dressing containing berberine for diabetic foot ulcer healing: in vitro and in vivo studies. Scientific Reports. 2020; 10(1):8312. [DOI:10.1038/s41598-020-65268-7] [PMID] [PMCID]

[17] Tsekova PB, Spasova MG, Manolova NE, Markova ND, Rashkov IB. Electrospun curcumin-loaded cellulose acetate/polyvinylpyrrolidone fibrous materials with complex architecture and antibacterial activity. Materials Science & Engineering. C, Materials for Biological Applications. 2017; 73:206-14. [DOI:10.1016/j.msec.2016.12.086] [PMID]

[18] Derakhshani A, Hesaraki S, Nezafati N, Azami M. Wound closure, angiogenesis and antibacterial behaviors of tetracalcium phosphate/hydroxyethyl cellulose/hyaluronic acid/gelatin composite dermal scaffolds. Journal of Biomaterials Science. Polymer Edition. 2022; 33(5):605-26. [DOI:10.1080/09205063.2021.2008786] [PMID]

[19] Yekta Tajhiz. TRIzol reagent, product manual. Tehran: Yekta Tajhiz Co. 2022.

[20] Pars Tous. cDNA synthesis kit instruction manual. Mashhad: Pars Tous Co. 2022.

[21] Pathak P, Nagarsenker M. Formulation and evaluation of lidocaine lipid nanosystems for dermal delivery. AAPS PharmSciTech. 2009;10(3):985-92. [DOI:10.1208/s12249-009-9287-1] [PMID] [PMCID]

[22] Chen PC, Huang JW, Pang J. An investigation of optimum nlc-sunscreen formulation using taguchi analysis. Journal of Nanomaterials. 2013; 2013(1):463732. [DOI:10.1155/2013/463732]

[23] Zheng Q, Xi Y, Weng Y. Functional electrospun nanofibers: Fabrication, properties, and applications in wound-healing process. RSC Advances. 2024; 14(5):3359-78. [DOI:10.1039/d3ra07075a] [PMID] [PMCID]

[24] Nequt I, Dorcioman G, Grumezescu V. Scaffolds for wound healing applications. Polymers (Basel). 2020; 12(9):2010. [DOI:10.3390/polym12092010] [PMID] [PMCID]

[25] Samadian H, Salehi M, Farzamfar S, Vaez A, Ehterami A, Sahrapeyma H, et al. In vitro and in vivo evaluation of electrospun cellulose acetate/gelatin/hydroxyapatite nanocomposite mats for wound dressing applications. Artificial Cells, Nanomedicine, and Biotechnology. 2018; 46(sup1):964-74. [DOI:10.1080/21691401.2018.1439842] [PMID]

[26] Rieger KA, Birch NP, Schiffman JD. Designing electrospun nanofiber mats to promote wound healing—A review. Journal of Materials Chemistry B. 2013; 1:4741-57. [Link]

[27] Khabbaz B, Solouk A, Mirzadeh H. Polyvinyl alcohol/soy protein isolate nanofibrous patch for wound-healing applications. Progress in Biomaterials. 2019; 8(3):185-96. [DOI:10.1007/s40204-019-00120-4] [PMID] [PMCID]

[28] Kaya S, Derman S. Properties of ideal wound dressing. Journal of Faculty of Pharmacy of Ankara University. 2023; 47(3):1119-31. [DOI:10.33483/jfpau.1253376]

[29] Suresh A, Shetty SS, Singh BN. Generation and evaluation of polycaprolactone/gelatin based porous-fibrous scaffolds through a layer-by-layer approach for wound healing. International Journal of Polymeric Materials and Polymeric Biomaterials. 2026; 75(6):683-96. [DOI:10.1080/00914037.2025.2598769]

[30] Robles KN, Zahra FT, Mu R, Giorgio T. Advances in electrospun poly(ε-caprolactone)-based nanofibrous scaffolds for tissue engineering. Polymers (Basel). 2024; 16(20):2853. [DOI:10.3390/polym16202853] [PMID] [PMCID]

[31] Aho IM, Agunwamba JC. Use of water extract of moringa oleifera seeds (WEMOS) in raw water treatment in makurdi, Nigeria. Global Journal of Engineering Research. 2015; 3(1):41–5. [DOI:10.4314/gjer.v13i1.5]

[32] Has C, Kiritsi D. Therapies for inherited skin fragility disorders. Experimental Dermatology. 2015; 24(5):325-31. [DOI:10.1111/exd.12666] [PMID]

[33] Erdoğmuş SF, Altintaş ÖE, Demirel HH, Okumuş N. Fabrication of wound dressings: Herbal extract-loaded nanoliposomes embedded in fungal chitosan/polycaprolactone electrospun nanofibers for tissue regeneration. Microscopy Research and Technique. 2024; 87(2):360-72. [DOI:10.1002/jemt.24438] [PMID]

[34] T A, Prabhu A, Baliga V, Bhat S, Thenkondar ST, Nayak Y, Nayak UY. Transforming wound management: nanomaterials and their clinical impact. Pharmaceutics. 2023; 15(5):1560. [DOI:10.3390/pharmaceutics15051560] [PMID]

[35] Rezvani Ghomi E, Khalili S, Nouri Khorasani S, Esmaeely Neisiany R, Ramakrishna S. Wound dressings: Current advances and future directions. Journal of Applied Polymer Science. 2019; 136(27):47738. [DOI: 10.1002/app.47738]

[36] Li YY, Ji SF, Fu XB, Jiang YF, Sun XY. Biomaterial-based mechanical regulation facilitates scarless wound healing with functional skin appendage regeneration. Military Medical Research. 2024; 11(1):13. [DOI10.1186/s40779-024-00519-6] [PMID]

[37] Xu YB, Chen GL, Guo MQ. Antioxidant and anti-inflammatory activities of the crude extracts of moringa oleifera from kenya and their correlations with flavonoids. Antioxidants (Basel). 2019; 8(8):296. [DOI:10.3390/antiox8080296] [PMID]